

# Automatic universal taxonomies for multi-domain semantic segmentation

**Petra Bevandić and Siniša Šegvić**  
 Faculty of Electrical Engineering and Computing  
 University of Zagreb  
 Zagreb, Croatia  
 name.surname@fer.hr

## Abstract

Training semantic segmentation models on multiple datasets has sparked a lot of recent interest in the computer vision community. This interest has been motivated by expensive annotations and a desire to achieve proficiency across multiple visual domains. However, established datasets have mutually incompatible labels which disrupt principled inference in the wild. We address this issue by automatic construction of universal taxonomies through iterative dataset integration. Our method detects subset-superset relationships between dataset-specific labels, and supports learning of sub-class logits by treating super-classes as partial labels. We present experiments on collections of standard datasets and demonstrate competitive generalization performance with respect to previous work.

## 1 Introduction

Semantic segmentation is an important computer vision task with exciting applications in intelligent transportation [14], medical diagnostics [25], remote surveillance [4], and autonomous robots [13]. Current state of the art is based on strongly supervised learning which implies a strong dependence on dense semantic ground truth. Unfortunately, producing dense annotations requires a lot of time and money [6, 43]. There are several datasets of intermediate size [24, 21, 37, 41], but none that is sufficient for delivering robust performance in the wild [37]. Thus, training across several datasets and domains appears as an attractive research direction.

A simple baseline involves per-dataset heads over shared features [9, 15]. Per-dataset predictions can be recombined into a common taxonomy [42], however this is not easily adapted to multi-class problems and overlapping taxonomies [20, 23, 39]. Another baseline concatenates per-dataset taxonomies [9, 22] and feeds them to common softmax. However, this may entail capacity loss due to competition between related logits. A recent approach reconciles a set of taxonomies by pragmatic label adaptation [18]. However, an ideal solution should retain all possible classes and require no relabeling. This can be done with hand-crafted universal taxonomies where superclasses promote recognition of subclasses and vice versa [2, 20, 23].

This paper makes a step further by considering automatic universal taxonomies over incompatible datasets as sketched in Figure 1. Our method hypothesizes cross-dataset relations through analysis. These hypotheses are evaluated against each other according to mIoU performance on all training datasets. We perform experiments on collections of large semantic segmentation datasets such as Vistas, Ade20k, COCO and WildDash 2. The recovered automatic taxonomies perform comparably to their manual counterparts [2] while outperforming all other baselines [18] by a considerable margin.

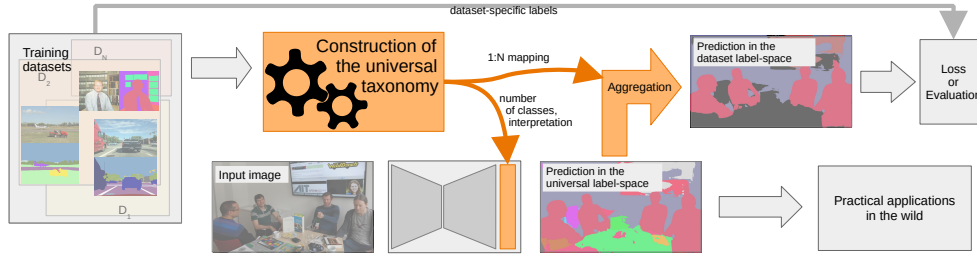


Figure 1: We consider automatic construction of a universal taxonomy from multiple datasets with incompatible labels (orange box). Our method recovers a set of disjoint universal classes, and accompanying 1:N mappings which connect dataset-specific and universal taxonomies. These mappings enable training and evaluation on original labels (top-right). The universal model can be exploited for interpretable inference in the wild (bottom-right).

## 2 Related work

We consider semantic segmentation for natural scene understanding (sec. 2.1) by studying cross-domain models which transcend particular training taxonomies (sec. 2.2). We focus on automatic construction of universal taxonomies (sec. 2.3).

### 2.1 Semantic segmentation

Semantic segmentation classifies each input pixel into one of  $C$  known classes [8, 29]. It is one of the most computationally intensive computer vision tasks due to high output resolution. The training footprint often constrains the model capacity [27]. Huge computational complexity leads to very long training times. Consequently, efficient models [12, 26, 25] and knowledge transfer [10] are a good fit for large cross-domain experiments. Besides faster training, they also improve accessibility and decrease environmental impact [28].

### 2.2 Cross-domain training

Early cross-domain training approaches do not incorporate relations between individual taxonomies. Instead, they either use separate dataset-specific prediction heads on top of shared features [16], or train on a concatenation of particular taxonomies [22]. Naive concatenation has been improved by encouraging cross-talk between logits [9].

Training dense open-set recognition models on positive and negative data may improve detection of unknown [5, 3] or novel classes [32]. This can be viewed as asymmetrical cross-domain training. The positive domain corresponds to the primary recognition task (e.g. road driving) while the negative domain typically corresponds to anomalies [5, 1, 31].

Some cross-domain approaches propose hierarchical universal taxonomies with distinct nodes for categories and classes [20, 23]. However, this requires complex learning procedures while not offering advantages over flat universal taxonomies.

Incompatible datasets can be unified under a custom common taxonomy by manual relabeling and removal of subclasses [18, 38]. However, these modifications are tedious and destructive. The more datasets one converts, the harder it gets to extend the common taxonomy with new subclasses. This issue can be elegantly solved by constructing a special taxonomy where each dataset-specific class can be expressed as a union of universal classes [2]. In this case, universal logits can be trained with respect to dataset-specific labels (cf. Figure 1) since dataset posteriors correspond to sums of universal posteriors [7]. The result of such construction can be referred to as universal taxonomy since it allows principled cross-dataset training without any modification of the original datasets. We extend this approach by considering automatic construction of such universal taxonomy from datasets with differing granularities.

### 2.3 Automatic construction of universal taxonomies

Manual resolution of dataset discrepancies is error prone, especially when the ambition is to train on multiple large-scale datasets with hundreds of symbolic labels. This issue can be elegantly circumvented by expressing semantic labels with text embeddings instead of categorical distributions [19, 35]. However, a recent study reveals that label semantics often vary across datasets. Their experiments suggest that visual cues outperform label semantics as a tool for recovering cross-dataset relations [33].

Recent work constructs an automatic taxonomy for object detection [42]. Their approach starts by training a model with shared features and separate prediction heads [9, 15]. Subsequently, they jointly re-train the object detectors while identifying corresponding classes across datasets through linear programming. The resulting cross-dataset mappings outperform their text-embedding counterparts. However, this approach does not handle subset/superset relationships and therefore does not produce a true taxonomy when dataset-specific classes happen to overlap. This situation hampers multi-class performance due to competition between related logits [2].

Cross-dataset relations have also been recovered according to class names [18]. In this setup, superclass logits can be trained with subclass labels [17]. However, this setup can not accommodate the standard multi-class loss, fails if there is a name mismatch [33, 42], and cannot train subclass logits with superclass labels.

Different than all previous work, our method constructs the only flat universal taxonomy which retains all labels in presence of subclass/superset relations.

## 3 Method

We consider automatic recovery of a flat universal taxonomy for a given collection of datasets in order to allow cross-domain training of dense prediction models. Our method discovers hierarchical relations between datasets by analyzing statistics of naive concatenation models. We construct pairwise taxonomies by hypothesizing and testing relations between pairs of classes from different datasets. We extend this procedure for arbitrary tuples of datasets through tournament-style iteration.

We transparently train our universal models by treating original annotations as partial labels. Occasionally, these models will predict classes which are disjoint from the native taxonomy of the input image. We denote such occurrences as foreign or extra-domain predictions. Conversely, predictions which fall within the native taxonomy are denoted as intra-domain predictions.

### 3.1 Post-inference mapping of a naive concatenation model

Naive concatenation is a pseudo-taxonomy which we obtain by simply concatenating individual taxonomies. We use the term pseudo-taxonomy since its member classes are not guaranteed to be disjoint (e.g. City-car and Vistas-car). Such overlaps require discrimination of semantically related classes and consequently diminish the effective model capacity.

We choose to avoid penalizing foreign predictions by performing post-inference mapping towards the naive input taxonomy. We define the unnormalized classification score of a particular native class  $S(c_i^a)$  as the sum of the correct posterior  $P(c_i^a)$  and posteriors of intersecting foreign classes  $P(c_j^b)$  [2]:

$$S(c_i^a) = P(c_i^a) + \sum_{c_i^a \cap c_j^b \neq \emptyset} P(c_j^b) \quad (1)$$

The expression  $c_i^a \cap c_j^b \neq \emptyset$  is true when some pixels labeled as  $c_i^a$  in dataset  $a$  would be labeled as  $c_j^b$  in dataset  $b$ . Consider a naive concatenation Cityscapes || Vistas, and assume the resulting model is evaluated on Cityscapes. Then, we would have:  $S(\text{city-car}) = P(\text{city-car}) + P(\text{vistas-car})$ . The model prediction corresponds to  $\text{argmax}_i S(c_i^a)$ .

We shall use unnormalized classification score 1 to test hypothesized overlap between particular pairs of labels in different datasets. Figure 2 shows that knowing which dataset-specific labels have a non-empty overlap brings us pretty close to the desired universal taxonomy.

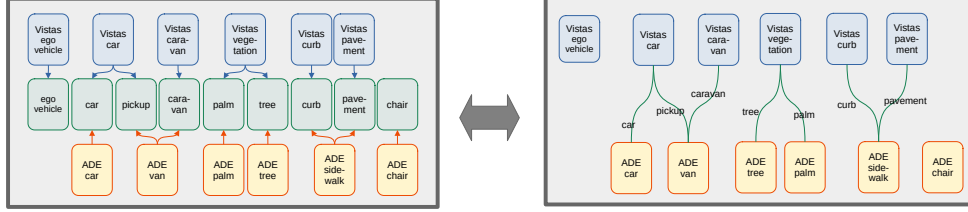


Figure 2: We can use the universal taxonomy (left) to find out which dataset-specific classes have a non-empty overlap. We can use information about cross dataset overlap (right) to recover a universal taxonomy.

### 3.2 Universal taxonomy for two datasets

Let us consider two datasets as  $D_a = \{c_i^a\}$  and  $D_b = \{c_j^b\}$ . Assume we train a naive concatenation model over  $D_a$  and  $D_b$  with  $C = |D_a| + |D_b|$  classes. We apply the model to the two training splits and collect between ground-truth classes and strongest activations of foreign classes. We represent this with matrices  $|D_a| \times |D_b|$  and  $|D_b| \times |D_a|$ . We use these matrices to hypothesize relations between classes. Note that we could have also analyzed cross-dataset predictions of single-dataset models [33]. We have conjectured that naive concatenation may work better due to the absence of domain shift. For each ground-truth class we consider the most common foreign prediction as a potential superclass. This forms a bipartite graph with  $C$  vertices which represent classes, and  $C$  edges pointing from a ground-truth class to its most frequent foreign prediction. Hence, each vertex has exactly one outgoing edge as illustrated in Figure 3 for ADE20K and Vistas. We only consider the most common prediction in order to increase statistical power and reduce the number of hypotheses and hyper-parameters.

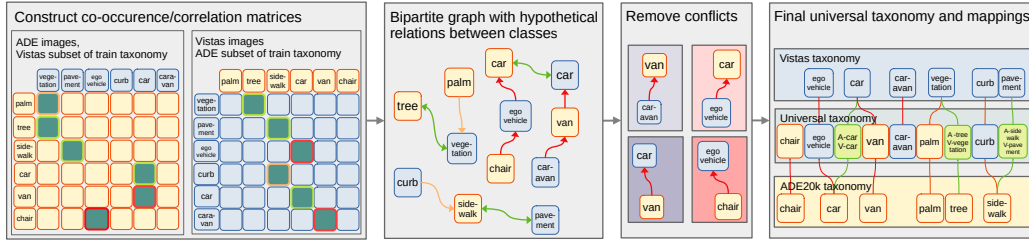


Figure 3: Our method collects two confusion matrices (left) between the ground truth (rows) and foreign predictions (columns). For each row, we locate the strongest column and form a bipartite graph (center-left). We note 3 2-cycles (green), 2 asymmetric relationships (orange), 2 and inconsistent triplets (red). We form pairs of conflicting hypotheses (shades of the same color, center right) and resolve them by testing on the training dataset (cf. Figure 4). The collected evidence allow us to recover the universal taxonomy (right).

We analyze the bipartite graph as follows. Cycles of length 2 ( $c_i^a \rightarrow c_j^b \rightarrow c_i^a$ ) get merged into two-way edges. Asymmetric relationships ( $c_i^a \rightarrow c_j^b$ ) suggest a subset hypothesis  $c_j^b \subset c_i^a$ . Inconsistent triplets  $c_i^a \rightarrow c_j^b \rightarrow c_k^a$  where  $c_k^a \not\rightarrow c_j^b$  suggest a subset and a superset hypothesis  $c_j^b \subset c_i^a \wedge c_k^a \supset c_j^b$ . This would mean that  $c_i^a \cap c_k^a \neq \emptyset$ , which is impossible since input datasets have proper taxonomies. We consider  $c_i^a \subset c_j^b$  and  $c_j^b \subset c_k^a$  as competing hypotheses which we evaluate according to the segmentation score (cf. Equation 1). We choose the hypothesis with the highest train mIoU performance averaged over the involved datasets. The resolution involves  $2N$  automatic evaluations where  $N$  denotes the number of conflicting pairs. Figures 3 and 4 illustrate this procedure for ADE20K and Vistas.

We recover the final universal taxonomy from the disambiguated bipartite graph (cf. Figure 4, right). Note that each universal class can be associated with all incident dataset-specific classes. We thus base the names of universal classes on associated dataset-specific class names: a one-way edge inherits the name of its source vertex, while a two-way edge inherits the names of both adjacent



vertices (cf. Figure 3, right). In our results, we use a diagonal line to form a two-way edge name: e.g. if  $\text{city} - \text{car} \rightarrow \text{vistas} - \text{car}$  and  $\text{vistas} - \text{car} \rightarrow \text{city} - \text{car}$ , we would have a universal class named 'city-car/vistas-car'. Our naming convention provides a degree of interpretability to resulting universal models.

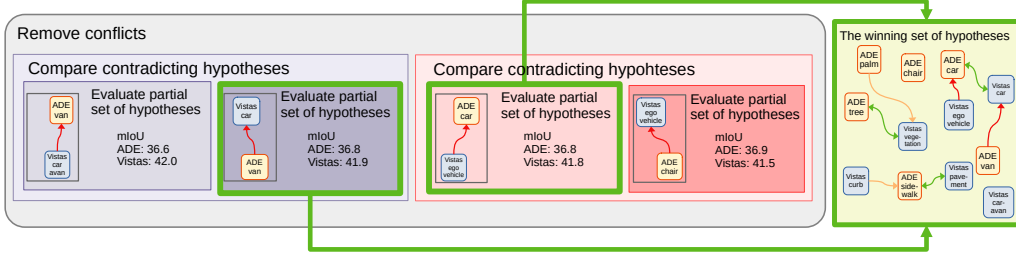


Figure 4: Resolution of contradicting hypotheses over dataset-specific labels. The winning hypotheses are selected by evaluation of the classification score (1) on the train dataset. Our evaluation procedure proceeds pair by pair and requires  $2 \cdot N$  evaluations.

### 3.3 Universal taxonomy for more than two datasets

Recovering a pairwise universal taxonomy allows us to unify the two involved datasets. The resulting meta-dataset contains images from the two datasets and partial labels in form of unions of universal classes. We can proceed by unifying this meta-dataset with subsequent datasets. However, lack of proper ground-truth precludes recovery of the proposed confusion matrix. We therefore approximate the confusion matrix with co-incidence between intra-domain and foreign predictions of the naive concatenation model.

To recover a universal taxonomy for more than two datasets, we proceed iteratively. We start by forming pairwise universal taxonomies. We then train naive concatenation models over pairs of meta-datasets and use them to unify the involved meta-datasets. We formulate mapping functions for original datasets as compositions of intermediate mapping functions.

The proposed procedure can be applied to any number of datasets in a straight-forward manner. We have successfully applied this procedure to the MSeg dataset collection.

## 4 Experiments

We train semantic segmentation models in multi-domain setups. We promote efficient experimentation [28] by leveraging pyramidal SwiftNet [26] with three shared ResNet-18 [11] backbones and ImageNet pre-training (SNp-rn18). We train on automatic universal taxonomies with partial labels [7, 39, 2]. We train naive concatenation models with the standard NLL loss. Both losses prioritize pixels at semantic boundaries [40]. We perform early stopping with respect to average mIoU validation performance. We attenuate the learning rate between  $5 \cdot 10^{-4}$  and  $6 \cdot 10^{-6}$  through cosine annealing. We evaluate by mapping foreign predictions to the void class [6].

We train on random crops of  $512 \times 512$  (§4.2 and §4.3) or  $768 \times 768$  pixels (§4.1) with horizontal flipping and random scaling between  $0.5 \times$  and  $2 \times$ . We favour crops with rare classes and form batches with even representation of all datasets. Our universal models were trained on one Tesla V100 32GB. We train naive concatenation models on two GPUs in order to ensure the same batch size across considered dataset collections. We construct universal taxonomies by analyzing only the training subsets.

### 4.1 Unifying dataset pairs

Table 1 presents experiments on pairs of datasets with incompatible taxonomies. All models are trained for 100 epochs. We compare the performance of our automatic taxonomies to the naive concatenation baseline and our manual universal taxonomies.

We first consider unifying Vistas [24] (road-driving, 65 classes) and ADE20K [41] (photos, 150 classes). Our second experiment pairs Vistas with Wilddash 2 (WD2, road-driving, 25 classes) [37]. We split WD2 into minitrain and minival as in [2]. Vistas has a finer granularity than WildDash 2 with the exception of car types.

Our automatic universal taxonomy for ADE20k-Vistas has less training logits than its manual counterpart. This happens because our automatic method connects some classes that are kept separate in the manual taxonomy (e.g. connecting flags with banners or rail tracks with conveyor belts). Noisy connections might also explain the performance drop on WildDash 2. Nevertheless, failures are rare: our universal taxonomies outperform naive concatenation.

Interestingly, our automatic taxonomy outperforms the manual taxonomy on some rare classes in WD2-Vistas experiments. The biggest per-class improvements in automatic taxonomies occur due to associating wd-person to vistas-ground-animal, and wd-truck to vistas-trailer. The improved generalization suggests that those rare Vistas classes get more training signal due to association with frequent WildDash classes.

We further consider the use of coincidence matrices instead of confusion matrices. The two approaches perform similarly, although their universal taxonomies differ.

Taxonomy	(ADE20K-Vistas)				(WD2-Vistas)			
	#	evals	ADE	Vistas	#	evals	WD2	Vistas
naive concat	215	N/A	36.8	41.1	98	N/A	54.8	42.8
manual univ.	186	N/A	37.4	42.7	67	N/A	56.2	44.4
auto univ. (conf.)	178	24	37.4	42.8	68	4	54.4	44.3
auto univ. (coinc.)	176	26	36.9	42.5	67	4	54.6	45.9

Table 1: Evaluation of joint training on ADE20K-Vistas and WildDash2-Vistas. Columns show the number of logits (#), number of tested hypotheses (evals) and mIoU performance on both datasets. Confusion and coincidence matrices perform comparably.

## 4.2 Merging multiple datasets

Table 2 evaluates our universal taxonomy over three datasets. We start from the universal taxonomy ADE20K-Vistas and extend it through unification with COCO (photos, 133 classes) [21]. Due to the size of the COCO dataset, we decrease the number of training epochs to 20. Before cropping, each image is resized so that its smaller side is 1080 pixels. We train our models on full training datasets, but only use the first 10000 images from each dataset for automatic construction of the universal taxonomy. The table shows that automatic universal taxonomy outperforms naive concatenation while substantially reducing the number of training classes.

Taxonomy	#	evals	ADE20K	Vistas	COCO
naive concatenation	348	N/A	30.7	32.7	36.5
manual univ. taxonomy	243	N/A	31.3	39.0	34.6
auto univ. taxonomy	233	44	30.8	37.4	37.7

Table 2: Joint training on ADE20K, Vistas and COCO. Columns show the number of logits (#), number tested hypotheses (evals) and mIoU performance.

Figure 5 presents a qualitative comparison between our automatic taxonomy and naive concatenation. Our automatic taxonomy succeeds to actualize many good class connections, such as mapping ade-food to {ade-food/coco-donut, coco-pizza, coco-sandwich, coco-hot-dog, coco-carrot, coco-food-other}. Furthermore, it finds some coherent connections we did not initially consider in our manual taxonomy such as mapping 'ade-person' to {'vistas-bicyclist', 'vistas-person/ade-person/coco-person', 'coco-baseball glove', 'coco-tie'}.

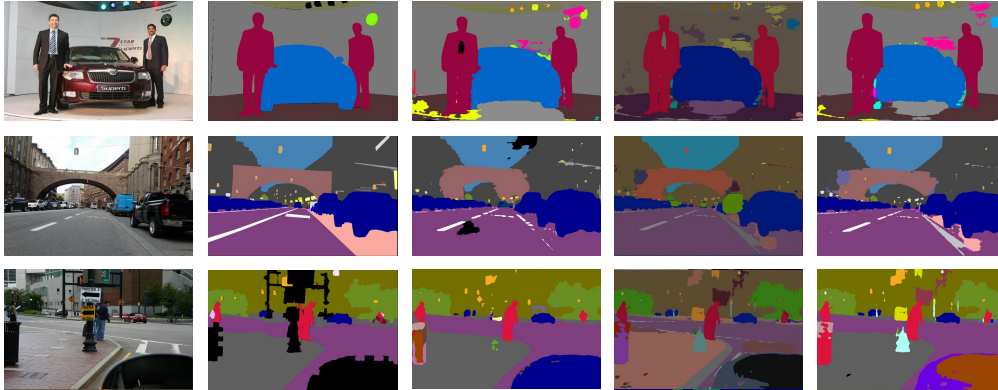


Figure 5: Qualitative comparison of cross-domain models on ADE20K (top), Vistas (middle) and COCO (bottom). We show the input image (column 1), ground truth labels (column 2), predictions of the naive concatenation model (column 3), and predictions of our model in universal (column 4) and dataset-specific labels (column 5). Naive concatenation introduces competition between logits that represent the same visual category. This triggers void predictions (black) on sky and road in the Vistas image. Our universal model finds universal classes that are not present in the corresponding dataset-specific taxonomy and connects them with correct dataset-specific classes: road-marking  $\rightarrow$  road and curb  $\rightarrow$  sidewalk in COCO, tie  $\rightarrow$  person in ADE20K and van  $\rightarrow$  car in Vistas.

### 4.3 Large-scale experiment on the MSeg dataset collection

MSeg dataset [18] collection encompasses ADE20K [41], BDD (19 classes) [36], Cityscapes (28 classes) [6], COCO [21], IDD (31 classes) [34], SUN RGBD (37 classes) [30] and Vistas [24]. Authors of the MSeg collection adapt all seven datasets towards a custom universal taxonomy of 194 classes. However, their taxonomy entails an omission of 61 classes in order to contain the relabeling effort. Note also that adding a new class to the MSeg taxonomy would require manual relabelling of all seven datasets.

We start the recovery by unifying dataset pairs: BDD-Cityscapes, IDD-Vistas, and ADE-COCO. We proceed by unifying BDD-City with IDD-Vistas, and ADE-COCO with SUN RGBD. Finally, we construct the universal taxonomy over all 7 datasets. If COCO is among the training datasets, we train for 20 instead of 100 epochs.

Table 3 compares our automatic universal taxonomy to the manual universal and MSeg taxonomies. Our automatic taxonomy performs comparably to the manual universal taxonomy [2] while outperforming MSEG taxonomy and naive concatenation. Our automatic taxonomy contains less classes than the manual universal taxonomy. This happens due to a few incorrect decisions on rare classes such as merging city-caravan, ade-washer and coco-toaster. Furthermore, our approach brings some debatable but arguably correct decisions due to visual similarity. Thus, vistas-pole is associated with bdd-pole/city-pole/vistas-pole/ade-pole, coco-baseball bat, coco-skis, sun-night-stand, and ade-column-pillar.

Interestingly, our approach finds some potentially valid connections that we did not initially consider in our manual taxonomy: it associates e.g. vistas-water to ade-swimming pool (there is often water in swimming pools), city-person to coco-handbag (people carry handbags) and bdd-fence to ade-cradle (cradles often have a safety fence).

## 5 Conclusion

We have presented a proof-of-concept for automatic construction of an interpretable universal taxonomy given a collection of multi-domain datasets with incompatible taxonomies. Our method outputs a set of mappings which connect dataset-specific classes with their universal counterparts. These mappings hierarchically connect concepts across particular taxonomies and equip universal

Taxonomy	#	evals	Ade20k	BDD	City	COCO	IDD	SUN	Vistas
naive concat.	469	N/A	27.0	55.6	69.0	29.8	51.3	37.4	33.7
manual univ. [2]	294	N/A	31.0	58.5	72.6	35.4	54.4	41.7	39.1
MSeg original	194	N/A	23.3	59.4	72.6	30.3	42.6	40.2	26.1
auto univ.	243	164	30.7	59.6	72.7	35.6	55.2	42.3	35.8

Table 3: Multi-domain performance evaluation (mIoU %) on the MSeg collection [18]. Unlike [18], we perform evaluation on all classes from the original dataset taxonomies as in [2].

models with a degree of interpretability. Our taxonomies allow training in the universal label space by treating dataset-specific classes as partial labels.

Our construction approach proceeds by iterative pairwise unification. The unification procedure operates by testing hypothesized relationships between dataset specific classes. We create hypotheses by analyzing a bipartite graph between cross-domain and intra-domain predictions of a naive concatenation model. We test hypotheses by comparing mIoU performance of the resulting post-inference mappings on the two training datasets.

We evaluate our universal taxonomies in experiments on incompatible datasets. We consider collections of datasets from the same domain as well as from different domains. We use lightweight models to reduce the training time, yet still succeed to infer coherent relationships between classes. Our universal models can output predictions both in universal and dataset-specific label space without decreasing inference speed. The reduced number of training logits indicates that our models are more memory-efficient than ad-hoc alternatives.

Our automatic universal taxonomies outperform the naive concatenation baseline and perform comparably to manually designed taxonomies. They are also much more flexible than universal taxonomies designed for standard NLL loss [18, 38], since we can exploit the full training potential of a given dataset collection without any relabeling effort. We observe the best relative performance of our models in large-scale experiments.

Future work should examine ways of streamlining the universal taxonomy construction and explore alternatives for hypothesizing relationships between dataset specific classes.

## References

- [1] P. Bevandić, I. Krešo, M. Oršić, and S. Šegvić. Dense open-set recognition based on training with noisy negative images. *Image and Vision Computing*, 124:104490, 2022.
- [2] P. Bevandić, M. Oršić, I. Grubišić, J. Šarić, and S. Šegvić. Multi-domain semantic segmentation with overlapping labels. In *Proceedings of the IEEE/CVF Winter Conference on Applications of Computer Vision (WACV)*, pages 2615–2624, January 2022.
- [3] G. D. Biase, H. Blum, R. Siegwart, and C. Cadena. Pixel-wise anomaly detection in complex driving scenes. In *Computer Vision and Pattern Recognition, CVPR*, 2021.
- [4] A. Boguszewski, D. Batorski, N. Ziemba-Jankowska, T. Dziedzic, and A. Zambrzycka. Land-cover.ai: Dataset for automatic mapping of buildings, woodlands, water and roads from aerial imagery. *2021 IEEE/CVF Conference on Computer Vision and Pattern Recognition Workshops (CVPRW)*, pages 1102–1110, 2021.
- [5] R. Chan, M. Rottmann, and H. Gottschalk. Entropy maximization and meta classification for out-of-distribution detection in semantic segmentation. In *International Conference on Computer Vision, ICCV*, 2021.
- [6] M. Cordts, M. Omran, S. Ramos, T. Rehfeld, M. Enzweiler, R. Benenson, U. Franke, S. Roth, and B. Schiele. The cityscapes dataset for semantic urban scene understanding. In *Proceedings of the IEEE conference on computer vision and pattern recognition*, pages 3213–3223, 2016.
- [7] T. Cour, B. Sapp, and B. Taskar. Learning from partial labels. *The Journal of Machine Learning Research*, 12:1501–1536, 2011.
- [8] C. Farabet, C. Couprie, L. Najman, and Y. LeCun. Learning hierarchical features for scene labeling. *IEEE Trans. Pattern Anal. Mach. Intell.*, 35(8):1915–1929, 2013.

- [9] D. Fourure, R. Emonet, E. Fromont, D. Muselet, N. Neverova, A. Trémeau, and C. Wolf. Multi-task, Multi-domain Learning: application to semantic segmentation and pose regression. *Neurocomputing*, 2017.
- [10] K. He, R. B. Girshick, and P. Dollár. Rethinking imagenet pre-training. In *ICCV*, pages 4917–4926. IEEE, 2019.
- [11] K. He, X. Zhang, S. Ren, and J. Sun. Deep residual learning for image recognition. In *Proceedings of the IEEE conference on computer vision and pattern recognition*, pages 770–778, 2016.
- [12] Y. Hong, H. Pan, W. Sun, and Y. Jia. Deep dual-resolution networks for real-time and accurate semantic segmentation of road scenes. *CoRR*, abs/2101.06085, 2021.
- [13] P. Hu, F. Perazzi, F. C. Heilbron, O. Wang, Z. L. Lin, K. Saenko, and S. Sclaroff. Real-time semantic segmentation with fast attention. *IEEE Robotics and Automation Letters*, 6:263–270, 2021.
- [14] J. Janai, F. Güney, A. Behl, and A. Geiger. Computer vision for autonomous vehicles: Problems, datasets and state of the art. *Foundations and Trends® in Computer Graphics and Vision*, 12(1–3):1–308, 2020.
- [15] T. Kalluri, G. Varma, M. Chandraker, and C. Jawahar. Universal semi-supervised semantic segmentation. In *Proceedings of the IEEE International Conference on Computer Vision*, pages 5259–5270, 2019.
- [16] T. Kalluri, G. Varma, M. Chandraker, and C. Jawahar. Universal semi-supervised semantic segmentation. In *Proceedings of the IEEE International Conference on Computer Vision*, pages 5259–5270, 2019.
- [17] D. Kim, Y. Tsai, Y. Suh, M. Faraki, S. Garg, M. Chandraker, and B. Han. Learning semantic segmentation from multiple datasets with label shifts. *CoRR*, abs/2202.14030, 2022.
- [18] J. Lambert, Z. Liu, O. Sener, J. Hays, and V. Koltun. Mseg: A composite dataset for multi-domain semantic segmentation. In *CVPR*, 2020.
- [19] B. Li, K. Q. Weinberger, S. J. Belongie, V. Koltun, and R. Ranftl. Language-driven semantic segmentation. In *ICLR*, 2022.
- [20] X. Liang, H. Zhou, and E. Xing. Dynamic-structured semantic propagation network. In *CVPR*, pages 752–761, 2018.
- [21] T. Lin, M. Maire, S. J. Belongie, J. Hays, P. Perona, D. Ramanan, P. Dollár, and C. L. Zitnick. Microsoft COCO: common objects in context. In *ECCV*, pages 740–755, 2014.
- [22] S. Masaki, T. Hirakawa, T. Yamashita, and H. Fujiiyoshi. Multi-domain semantic-segmentation using multi-head model. In *2021 IEEE International Intelligent Transportation Systems Conference (ITSC)*, pages 2802–2807, 2021.
- [23] P. Meletis and G. Dubbelman. Training of convolutional networks on multiple heterogeneous datasets for street scene semantic segmentation. In *Intelligent Vehicles Symposium*, pages 1045–1050, 2018.
- [24] G. Neuhold, T. Ollmann, S. Rota Bulò, and P. Kotschieder. Mapillary vistas dataset for semantic understanding of street scenes. In *ICCV*, pages 5000–5009, 2017.
- [25] D. Nie, J. Xue, and X. Ren. Bidirectional pyramid networks for semantic segmentation. In *ACCV*, pages 654–671, 2020.
- [26] M. Oršić and S. Šegvić. Efficient semantic segmentation with pyramidal fusion. *Pattern Recognition*, page 107611, 2021.
- [27] S. Rota Bulò, L. Porzi, and P. Kotschieder. In-place activated batchnorm for memory-optimized training of dnns. In *Proceedings of the IEEE Conference on Computer Vision and Pattern Recognition*, pages 5639–5647, 2018.
- [28] R. Schwartz, J. Dodge, N. A. Smith, and O. Etzioni. Green AI. *Commun. ACM*, 63(12):54–63, 2020.
- [29] E. Shelhamer, J. Long, and T. Darrell. Fully convolutional networks for semantic segmentation. *IEEE Trans. Pattern Anal. Mach. Intell.*, 39(4):640–651, 2017.
- [30] S. Song, S. P. Lichtenberg, and J. Xiao. Sun rgb-d: A rgb-d scene understanding benchmark suite. In *CVPR*, pages 567–576, 2015.
- [31] Y. Tian, Y. Liu, G. Pang, F. Liu, Y. Chen, and G. Carneiro. Pixel-wise energy-biased abstention learning for anomaly segmentation on complex urban driving scenes. *CoRR*, abs/2111.12264, 2021.

- [32] S. Uhlemeyer, M. Rottmann, and H. Gottschalk. Towards unsupervised open world semantic segmentation. *CoRR*, abs/2201.01073, 2022.
- [33] J. Uijlings, T. Mensink, and V. Ferrari. The missing link: Finding label relations across datasets. *CoRR*, abs/2206.04453, 2022.
- [34] G. Varma, A. Subramanian, A. M. Namboodiri, M. Chandraker, and C. V. Jawahar. IDD: A dataset for exploring problems of autonomous navigation in unconstrained environments. In *WACV*, pages 1743–1751, 2019.
- [35] W. Yin, Y. Liu, C. Shen, A. van den Hengel, and B. Sun. The devil is in the labels: Semantic segmentation from sentences. *CoRR*, abs/2202.02002, 2022.
- [36] F. Yu, W. Xian, Y. Chen, F. Liu, M. Liao, V. Madhavan, and T. Darrell. BDD100K: A diverse driving video database with scalable annotation tooling. *arXiv preprint arXiv:1805.04687*, 2018.
- [37] O. Zendel, K. Honauer, M. Murschitz, D. Steininger, and G. Fernandez Dominguez. Wilddash - creating hazard-aware benchmarks. In *ECCV*, 2018.
- [38] O. Zendel, M. Schörghuber, B. Rainer, M. Murschitz, and C. Beleznaï. Unifying panoptic segmentation for autonomous driving. In *Proceedings of the IEEE/CVF Conference on Computer Vision and Pattern Recognition (CVPR)*, pages 21351–21360, June 2022.
- [39] X. Zhao, S. Schuster, G. Sharma, Y. Tsai, M. Chandraker, and Y. Wu. Object detection with a unified label space from multiple datasets. In *ECCV*, pages 178–193, 2020.
- [40] M. Zhen, J. Wang, L. Zhou, T. Fang, and L. Quan. Learning fully dense neural networks for image semantic segmentation. In *AAAI*, 2019.
- [41] B. Zhou, H. Zhao, X. Puig, S. Fidler, A. Barriuso, and A. Torralba. Scene parsing through ade20k dataset. In *CVPR*, pages 633–641, 2017.
- [42] X. Zhou, V. Koltun, and P. Krähenbühl. Simple multi-dataset detection. In *CVPR*, 2022.
- [43] A. Zlateski, R. Jaroensri, P. Sharma, and F. Durand. On the importance of label quality for semantic segmentation. In *CVPR*, pages 1479–1487, 2018.